

## UNIT-CELL PARAMETERS OF THE MICROCLINE-LOW ALBITE AND THE SANIDINE-HIGH ALBITE SOLID SOLUTION SERIES

PHILIP M. ORVILLE, *Yale University, New Haven, Connecticut.*

### ABSTRACT

Eleven compositions in the microcline-low albite solid solution were produced by dry homogenization at 900°C of mixtures of Ab-rich and Or-rich end members produced from a natural "maximum microcline" by cation exchange with molten alkali chlorides at 900°C. Twenty compositions in the sanidine-high albite solid solution were crystallized from glasses under hydrothermal conditions.

Unit-cell parameters were determined from X-ray powder data for both the microcline-low albite and the sanidine-high albite solid solutions by means of a least-squares refinement computer program.

The volume curves for both feldspar series show positive volumes of mixing. The maximum volume of mixing for the microcline-low albite series is 1.3 percent at Or<sub>50.6</sub> mole percent and for the sanidine-high albite series, 0.9 percent at Or<sub>55.1</sub> mole percent. Volume curves for the two series nearly coincide between Or<sub>100</sub> and Or<sub>20</sub>Ab<sub>80</sub> but more Ab-rich compositions show significantly lower volumes in the microcline-low albite solid solution.

The triclinic to monoclinic symmetry transformation in the sanidine-high albite solid solution occurs at  $43.5 \pm 2.0$  mole percent Or at room temperature.

Because unit-cell dimension  $a$  is nearly independent of structural state and strongly dependent on composition, it provides a useful measure of composition for alkali feldspars. For a given structural state, variation in  $a$  of about 0.004 Å corresponds to a composition variation of 1.0 percent Or. The maximum effect of Al:Si order on  $a$  is equivalent to the effect of 4 percent Or.

X-ray determinative curves for the microcline-low albite and the sanidine-high albite series are given in terms of spacings for the reflections (201) and (400), and  $\Delta 2\theta$  for the reflection (201) using KBrO<sub>3</sub> as an internal standard.

The trend of compositions as plotted on an  $\alpha$ - $\gamma$  diagram suggests that the microcline-low albite series prepared in this study is slightly less ordered than true "maximum" microcline but more ordered than most natural microcline specimens.

### INTRODUCTION

The physical properties of the alkali feldspars at room temperature and pressure depend upon both composition and ordering of Al and Si among the tetrahedral sites. It is now possible to prepare series of alkali feldspars of known composition and of constant Al:Si order. Such feldspars can then be studied directly to determine their physical properties. It is no longer necessary to hypothesize about the relative effects of "structural state" and composition on the physical properties of natural alkali feldspars.

### PREPARATION OF MICROCLINE-LOW ALBITE SOLID SOLUTIONS

It has not been possible to synthesize either microcline or low albite directly but it has been possible to convert one to the other by exchange of alkalis.

Laves (1951) produced microcline by heating natural low albite in the presence of glass of K-feldspar composition. He maintained, largely on the basis of this conversion, that microcline and low albite were structural analogues and that they were end members of a single solid solution series.

Wyart and Sabatier (1956) produced microcline from natural low albite by reaction with molten KCl and low albite from natural microcline by reaction with molten NaCl. When alkali exchange reactions were carried out under hydrothermal conditions, the products were sanidine and high albite.

Goldsmith and Laves (1961) reported the production of several intermediate compositions in the microcline-low albite solution series by heating mixtures of natural microcline and synthetic glass of  $\text{NaAlSi}_3\text{O}_8$  (Ab) composition and mixtures of natural low albite and synthetic glass of  $\text{KAlSi}_3\text{O}_8$  (Or) composition.

In the present study, Ab-rich and Or-rich end members of the microcline-low albite solid solution series were produced by alkali exchange of a natural microcline with molten alkali chlorides. Intermediate compositions in the solid solution series were made by dry heating mixtures of the end members. The advantages of preparing the feldspar end members and intermediate compositions in this way are:

- (1) A single, well-characterized natural feldspar starting material is used.
- (2) All intermediate members in the solid solution series can be produced, and their compositions can be either determined directly by chemical analysis or calculated from the known end member compositions.

*Natural feldspar samples.* The natural microcline used as a starting material was a portion of a single meter-sized microcline perthite crystal from the Hugo pegmatite, Black Hills, South Dakota. For a description of this pegmatite, see Norton, Page and Brobst (1962). The microcline sample was collected from zone 5 (quartz-microcline-spodumene intermediate zone) and is notable for its unusually low Ca-content (about 0.02 wt percent) and freedom from fine-grained sericitic alteration. Figure 1 is a photomicrograph of this microcline.

The microcline has well-developed grid twinning with twin lamellae generally 0.002–0.005 mm in thickness. Seven percent plagioclase is included within the microcline crystal, 5 percent as irregularly oriented laths up to 1 mm in size, and 2 percent in small optically continuous patches in apparent crystallographic continuity with the microcline host. Both types of plagioclase inclusions show polysynthetic albite twinning

with twin lamellae ranging from 0.03 to 0.3 mm in width. About 1 percent muscovite is present in subhedral laths and plates that average 0.3 mm in size. A few tenths percent quartz is present in anhedral equant grains averaging 0.5 mm in size.

Separation of the  $131\text{-}\bar{1}31$  powder diffraction peaks show this natural microcline to be nearly maximum microcline with a "triclinicity" (as defined by Goldsmith and Laves, 1954) of 0.94. Values of  $\alpha^*$  ( $90^\circ 23'$ ) and

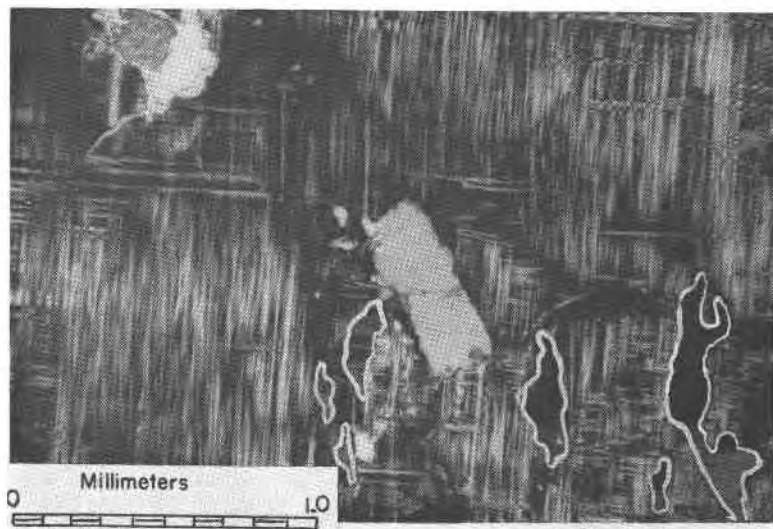


FIG. 1. Photomicrograph of Hugo microcline starting material. Thin section cut parallel to (001) cleavage, crossed polarizers. Plagioclase as irregular stringers (outlined in white) in parallel crystallographic orientation with microcline host and as blocky grain (center) with irregular crystallographic orientation. Muscovite in equant grains (upper left). Sieve fraction 100–200 mesh is about 0.1 mm diameter.

$\gamma^*$  ( $92^\circ 12'$ ) are close to the highest values reported for microcline by Laves (1952) and Mackenzie (1956).

As a preliminary treatment, the natural microcline starting material was crushed and sieved. Nearly all the muscovite impurity was retained on the 100 mesh sieve. All subsequent treatment of the feldspar was carried out on the 100–200 mesh fraction.

The bulk composition of the microcline starting material as determined by partial chemical analysis is  $\text{Or}_{85.7}\text{Ab}_{11.6}\text{An}_{0.2}\text{Rb-feldspar}_{2.4}$  (wt. percent), Table 1. Since approximately 7 percent plagioclase is present in the mode (see above and footnote (1), Table 1) the microcline matrix must contain about 5 percent of (Ab+An) in solid solution. The unit

TABLE 1. PARTIAL CHEMICAL ANALYSES OF ALKALI FELDSPARS

Material	Hugo Microcline <sup>1</sup>		Hugo Albite <sup>2</sup>	Low Albite		Microcline		
Treatment Sample	Untreated		Untreated	Hugo Microcline + NaCl		Hugo Microcline + NaCl + KCl		
	PMO-147-57-1	PMO-147-57-2	PMO 143-57	128-62	49-62 <sup>3</sup>	59-62	131-62	125-62
A.								
K	11.55	11.82	0.22	0.16	—	13.79	13.59	13.79
Na	0.98	1.00	8.06	8.82	—	0.036	0.030	0.030
Ca	0.028	0.026	0.030	.019	—	0.018	0.023	0.024
Rb	0.62	—	—	<.02	—	<0.02	—	—
B.								
Or	83.13		1.6	1.14	—	98.3	96.72	98.14
Ab	11.29		91.9	100.57	—	0.41	0.34	0.34
An	0.19		0.21	0.13	—	0.12	0.16	0.17
Rb-feld	2.36		—	<0.1	—	<0.1	—	—
	96.92		93.8	101.8		98.8	97.2	98.6
C.								
Or	85.72		1.7	1.21	0.93	99.47	99.48	99.48
Ab	11.64		97.9	98.75	98.88	0.41	0.35	0.34
An	0.20		0.22	0.13	0.19	0.12	0.16	0.17
Rb-feld.	2.43		—	—	—	—	—	—
	100.0		100.0	100.0	100.0	100.0	100.0	100.0
D.	Or <sub>88.7</sub> Ab <sub>11.6</sub> An <sub>0.2</sub> Rb-feld <sub>2.4</sub>		Or <sub>1.7</sub> Ab <sub>97.9</sub> An <sub>.2</sub>	Or <sub>1.6</sub> Ab <sub>98.8</sub> An <sub>0.2</sub>		Or <sub>99.5</sub> Ab <sub>0.3</sub> An <sub>0.2</sub>		

A. Cations as weight percent. Na, K and Rb by flame photometer. Ca by EDTA titration using glyoxal-bis-(2-hydroxyanil) as indicator (Goldstein, 1959).

B. Feldspar molecules as weight percent; calculated from cations.

C. Feldspar molecules summed to 100 weight percent.

D. Molecular formulas.

<sup>1</sup> Point count modal analysis of two thin sections (total count 1909 points) showed 6.9% plagioclase, 92.2% microcline and 0.9% muscovite. Essentially no muscovite was present in the 100–200 mesh fraction used in the salt-exchange experiments.

<sup>2</sup> Contains 2–5% muscovite and ~2% quartz impurities as estimated from X-ray powder pattern.

<sup>3</sup> Unknown amount of evaporation of sample solution 49-62 occurred before analysis. Relative concentrations of Na, K and Ca have been used to calculate feldspar molecules summed to 100 weight percent.

cell parameters and  $\bar{2}01$  peak position for the untreated microcline material suggest approximately 4 percent (Ab+An) in solid solution.

An albite sample was also collected from the Hugo pegmatite so that the products of the alkali chloride exchange could be directly compared with the feldspar phases that occur in close association in nature. The albite sample is from zone 4 (quartz-cleavelandite intermediate zone) and was collected from within five feet of the microcline sample. The albite occurs in bladed aggregates of cleavelandite habit with a small amount of intergrown quartz and muscovite. The albite is in lath-shaped

grains approximately 0.5 mm in minimum and 5 mm in maximum dimension elongate parallel to well-developed polysynthetic twinning. Partial chemical analysis (Table 1) and exchange treatment with KCl were carried out on a 100–200 mesh fraction of this albite sample. Mineral impurities are estimated from X-ray powder patterns to be 2–5 percent muscovite and about 2 percent quartz. The Ca-content is 0.03 wt percent, some of which may be present in minute apatite inclusions, which places an upper limit an An-content of 0.3 percent.

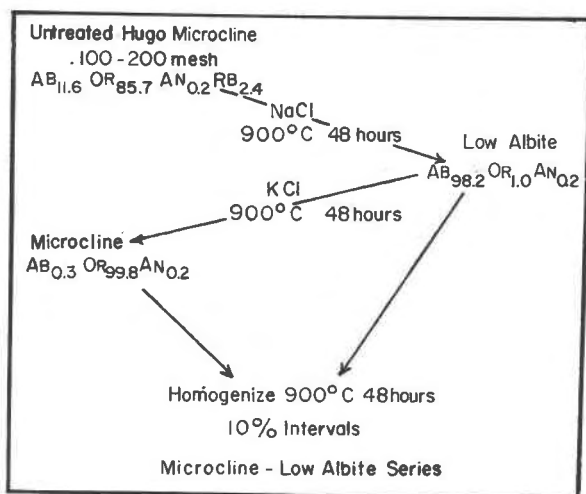


Fig. 2. Preparation of microcline-low albite series. Schematic flow sheet.

*Alkali Exchange and Homogenization Procedures.* The preparation scheme for producing microcline-low albite solid solution is shown diagrammatically in Figure 2. The natural microcline was reacted with 30 times its weight of NaCl at 900°C for 48 hours in a tightly covered platinum dish. Part of the nearly potassium-free albite thereby produced was reacted with 30 times its weight of KCl at 900°C for 48 hours to produce a nearly sodium-free and rubidium-free microcline. The size of platinum container available limited the amount of feldspar that could be treated at one time to about 3 grams. Partial chemical analyses of two batches after reaction with NaCl and three batches after reaction with both NaCl and KCl are given in Table 1.

The 100–200 mesh feldspar was separated by dissolving the salt in water, then decanting the solution. Several further washings and decantations left the feldspar free of alkali chloride. The decanted alkali chloride-bearing solution was filtered through a 0.3 micron Millipore filter to

determine if fine-grained reaction products were present. About 10 milligrams of material was normally retained on the filter. The X-ray powder pattern of this material was identical with that of the 100–200 mesh feldspar material with the addition only of the one or two strongest peaks of metallic platinum. Examination with the microscope showed only feldspar cleavage fragments and very sparse metallic globules 5 to 10 microns in diameter, presumably of platinum.

Mixtures of the pure (or nearly so) end members were made up at 10 percent intervals and were homogenized dry at 900°C for 48 hours.<sup>1</sup> Rate studies of the homogenization process showed that homogenization was effectively complete after 24 hours, as demonstrated by a single sharp 201 X-ray diffraction peak.

#### PREPARATION OF SANIDINE-HIGH ALBITE SOLID SOLUTIONS

The unit-cell parameters of the sanidine-high albite series were determined by Donnay and Donnay (1952). Because even very small differences in unit cell parameters may be significant in interpreting relationships between unit-cell dimensions, composition and degree of ordering in the alkali feldspars, it seemed desirable to redetermine the unit-cell dimensions for the sanidine-high albite series, using the same X-ray and computational methods as for the microcline-low albite series. The greater number of compositions used in this study and the use of computer techniques in processing the data should lead to a more precise definition of the relationship between composition and unit-cell parameters in the sanidine-high albite series.

Twenty alkali feldspar compositions were crystallized hydrothermally from glasses prepared by J. F. Schairer at the Geophysical Laboratory, Carnegie Institution of Washington. Crystallization was at 800°C, 1000 bars H<sub>2</sub>O pressure for 5 or 7 days in sealed platinum tubes. In the study of Donnay and Donnay, 1952, crystallization was carried out at 1000 kg/cm<sup>2</sup> H<sub>2</sub>O pressure and 700°C for some compositions and 800°C for others, and crystallization times varied from one to nine days.

#### DETERMINATION OF UNIT-CELL PARAMETERS

Each alkali feldspar sample was finely ground and prepared as a smear mount on a glass slide. Finely ground and annealed (48 hours at 700°) reagent grade CaF<sub>2</sub> was added to each smear mount as an internal standard. Three X-ray powder patterns were run for each composition on a

<sup>1</sup> It is important that the homogenization and the molten salt treatment be carried out in nonreactive containers. The salt vapor as well as the molten salt itself, will react with, among many other materials, sintered alumina. Homogenization runs carried out in silver capsules at 900°C produced dirty gray feldspar that was not used further in this study.

Siemens Crystalloflex 4 diffractometer using copper radiation at  $\frac{1}{8}^\circ/\text{min}$  scan rate, a source aperture of  $1^\circ$  and a detector aperture of 0.2 mm.

Peak positions were measured at the estimated center line of the top 1/10 of each peak. The (111) and (220) X-ray reflections of the  $\text{CaF}_2$  internal standard were included in each pattern and were measured in the same way as the feldspar peaks. The absolute  $2\theta$  values for the  $\text{CaF}_2$  peaks were calculated for  $\text{CuK}\alpha_1$  radiation using the unit cell dimension  $\text{CaF}_2$  ( $a=5.4620$ ) as determined by D. Wones (written communication) at the U. S. Geological Survey.

Peaks were ranked according to visual and statistical quality following a scheme proposed by T. Wright (written communication).

### *I. Visual Quality*

- A: Sharp peaks whose upper 1/10 is confined to  $0.1^\circ 2\theta$
- B: Broader peaks whose upper 1/10 is broader than  $0.1^\circ 2\theta$
- C: Very broad peaks, peaks having strong interference from adjacent peak or very indistinct peaks of low intensity.

### *II. Statistical Quality*

Peaks in which the spread of measurement on 3 charts is

- A: less than or equal to  $0.015^\circ 2\theta$
- B: greater than  $0.015^\circ$  but less than or equal to  $0.03^\circ 2\theta$
- C: greater than  $0.03^\circ 2\theta$
- D: not measurable on all three charts

The criteria for dropping peaks from the initial refinement were as follows:

- (1) All peaks of C-C or D quality.
- (2) All peaks which do not appear on at least 3 consecutive or 4 total compositions.

From 25 to 40 satisfactory peaks could be measured for each chart for each composition in the range  $13^\circ$  to  $53^\circ 2\theta$ . These unindexed peak measurements were processed at the U. S. Geological Survey by D. B. Stewart by the least squares unit cell refinement program developed by Appleman, Evans and Handwerker (1963). This program gives both a unit cell and an indexing of peaks based on that unit cell.

The tentative computer indexing of peaks was combined with an inspection of the charts for all members of the solid solution series to decide which peaks were unambiguously indexed and did not interfere with one another. The number of single, definitely indexed peaks ranged from 8 to 29.

A least squares unit-cell refinement using only single well-indexed lines was run on the computer for each composition using the fixed index

TABLE 2A. DIRECT UNIT-CELL PARAMETERS, MICROCLINE-LOW ALBITE SERIES

Composition			Lines	$a$		$b$	$c$	$\alpha$		$\beta$		$\gamma$		Volume	
Sample	wt% Or	mole% Or		$\text{\AA}$	$\text{\AA}$			deg.	min.	deg.	min.	deg.	min.	$\text{\AA}^3$	cm <sup>3</sup> /mol
128-62	1.00	0.94	14	8.1421 $\pm$ 0.0032	12.7807 $\pm$ 0.0043	7.1554 $\pm$ 0.0018	94	4.99 $\pm$ 2.71	116	40.45 $\pm$ 2.11	87	50.84 $\pm$ 2.70	663.67 $\pm$ 0.31	99.92 $\pm$ 0.05	
55-63	10.85	10.27	11	8.1808 $\pm$ 0.0036	12.7967 $\pm$ 0.0103	7.1622 $\pm$ 0.0019	93	48.83 $\pm$ 3.92	116	32.64 $\pm$ 2.47	87	46.32 $\pm$ 4.18	669.23 $\pm$ 0.53	100.76 $\pm$ 0.08	
157-63	20.70	19.71	9	8.2319 $\pm$ 0.0033	12.8442 $\pm$ 0.0024	7.1749 $\pm$ 0.0011	93	10.50 $\pm$ 2.10	116	21.75 $\pm$ 1.06	87	46.30 $\pm$ 1.58	678.60 $\pm$ 0.25	102.17 $\pm$ 0.04	
49-63	30.55	29.27	8	8.2848 $\pm$ 0.0020	12.8848 $\pm$ 0.0014	7.1894 $\pm$ 0.0006	92	39.80 $\pm$ 1.48	116	25.58 $\pm$ 2.48	87	48.42 $\pm$ 1.28	686.38 $\pm$ 0.30	103.34 $\pm$ 0.05	
51-63	40.40	38.96	11	8.3374 $\pm$ 0.0030	11.9071 $\pm$ 0.0036	7.1971 $\pm$ 0.0015	91	56.79 $\pm$ 3.73	116	6.16 $\pm$ 3.85	87	37.88 $\pm$ 1.62	694.80 $\pm$ 0.35	104.61 $\pm$ 0.05	
158-63	50.25	48.76	13	8.3808 $\pm$ 0.0040	12.9231 $\pm$ 0.0043	7.2019 $\pm$ 0.0019	91	34.03 $\pm$ 2.96	116	1.20 $\pm$ 1.94	87	36.74 $\pm$ 1.86	700.30 $\pm$ 0.31	105.44 $\pm$ 0.05	
57-63	60.10	58.68	20	8.4197 $\pm$ 0.0016	12.9345 $\pm$ 0.0030	7.2060 $\pm$ 0.0014	91	10.78 $\pm$ 1.74	115	58.17 $\pm$ 1.12	87	39.56 $\pm$ 1.45	704.93 $\pm$ 0.20	106.14 $\pm$ 0.03	
50-63	69.95	68.71	19	8.4715 $\pm$ 0.0016	12.9501 $\pm$ 0.0029	7.2124 $\pm$ 0.0014	90	59.28 $\pm$ 2.04	115	55.26 $\pm$ 1.18	87	36.82 $\pm$ 1.48	711.04 $\pm$ 0.21	107.06 $\pm$ 0.03	
156-63	79.80	78.86	20	8.5091 $\pm$ 0.0020	12.9545 $\pm$ 0.0026	7.2141 $\pm$ 0.0013	90	44.72 $\pm$ 1.64	115	52.06 $\pm$ 1.10	87	44.45 $\pm$ 1.31	714.98 $\pm$ 0.19	107.65 $\pm$ 0.03	
56-63	89.65	89.11	16	8.5466 $\pm$ 0.0020	12.9552 $\pm$ 0.0021	7.2160 $\pm$ 0.0009	90	40.16 $\pm$ 1.30	115	55.25 $\pm$ 1.10	87	45.08 $\pm$ 1.22	718.03 $\pm$ 0.16	108.11 $\pm$ 0.02	
131-62	99.50	99.48	16	8.5891 $\pm$ 0.0034	12.9628 $\pm$ 0.0038	7.2230 $\pm$ 0.0015	90	37.00 $\pm$ 2.78	115	57.12 $\pm$ 1.90	87	44.43 $\pm$ 2.24	722.52 $\pm$ 0.29	108.78 $\pm$ 0.04	
Hugo Microcline PMO 147-57															
			18	8.5774 $\pm$ 0.0025	12.9610 $\pm$ 0.0027	7.2199 $\pm$ 0.0015	90	38.25 $\pm$ 1.80	115	56.81 $\pm$ 1.10	87	44.81 $\pm$ 1.23	721.17 $\pm$ 0.21	108.58 $\pm$ 0.03	
Hugo Albite PMO 143-57															
			18	8.1378 $\pm$ 0.0012	12.7817 $\pm$ 0.0019	7.1572 $\pm$ 0.00078	94	14.64 $\pm$ 1.09	116	37.16 $\pm$ 0.66	87	41.69 $\pm$ 0.95	663.70 $\pm$ 0.12	99.93 $\pm$ 0.02	
Hugo Albite (KCl exchange)															
			26	8.5823 $\pm$ 0.0024	12.9644 $\pm$ 0.0028	7.2219 $\pm$ 0.0014	90	37.79 $\pm$ 1.43	115	55.53 $\pm$ 1.08	87	40.85 $\pm$ 1.39	722.07 $\pm$ 0.21	108.72 $\pm$ 0.03	



TABLE 2B. RECIPROCAL UNIT-CELL PARAMETERS, MICROCLINE-LOW ALBITE SERIES

sample	Composition		$a^*$ $1/\text{\AA}$	$b^*$ $1/\text{\AA}$	$c^*$ $1/\text{\AA}$	$\alpha^*$		$\beta^*$		$\gamma^*$ deg. min.
	wt% Or	mole% Or				deg.	min.	deg.	min.	
128-62	1.00	0.94	0.137448 $\pm$ 0.000038	0.0784434 $\pm$ 0.000028	0.156689 $\pm$ 0.000052	86	30.66 $\pm$ 2.37	63	24.26 $\pm$ 2.18	90 21.59 $\pm$ 2.42
55-63	10.85	10.27	0.136648 $\pm$ 0.000039	0.0783230 $\pm$ 0.000067	0.156311 $\pm$ 0.000065	86	50.92 $\pm$ 2.93	63	32.22 $\pm$ 2.61	90 35.25 $\pm$ 3.33
157-63	20.70	19.71	0.135598 $\pm$ 0.000053	0.0779860 $\pm$ 0.000015	0.155692 $\pm$ 0.000023	87	33.59 $\pm$ 1.98	63	42.62 $\pm$ 1.09	90 54.91 $\pm$ 1.43
49-63	30.55	29.27	0.134813 $\pm$ 0.000062	0.0777100 $\pm$ 0.000009	0.155409 $\pm$ 0.000056	88	6.90 $\pm$ 1.77	63	38.16 $\pm$ 2.49	91 7.59 $\pm$ 1.72
51-63	40.40	38.96	0.133622 $\pm$ 0.000053	0.0775548 $\pm$ 0.000022	0.154749 $\pm$ 0.000087	88	59.53 $\pm$ 4.27	63	56.81 $\pm$ 3.79	91 41.08 $\pm$ 2.83
158-63	50.25	48.76	0.132852 $\pm$ 0.000064	0.0774521 $\pm$ 0.000025	0.154522 $\pm$ 0.000046	89	25.26 $\pm$ 3.10	64	1.08 $\pm$ 1.96	91 53.54 $\pm$ 2.06
57-63	60.10	58.68	0.132170 $\pm$ 0.000033	0.0773810 $\pm$ 0.000018	0.154339 $\pm$ 0.000042	89	49.65 $\pm$ 1.65	64	3.30 $\pm$ 1.13	92 1.75 $\pm$ 1.34
50-63	69.95	68.71	0.131341 $\pm$ 0.000026	0.0772862 $\pm$ 0.000017	0.154158 $\pm$ 0.000035	90	3.66 $\pm$ 2.08	64	5.78 $\pm$ 1.20	92 10.39 $\pm$ 1.51
156-63	79.80	78.86	0.130699 $\pm$ 0.000021	0.0772540 $\pm$ 0.000015	0.154055 $\pm$ 0.000029	90	16.02 $\pm$ 1.56	64	3.47 $\pm$ 1.10	92 8.96 $\pm$ 1.21
56-63	89.65	89.11	0.130187 $\pm$ 0.000024	0.0772500 $\pm$ 0.000013	0.154085 $\pm$ 0.000027	90	20.92 $\pm$ 1.18	64	5.10 $\pm$ 1.10	92 10.50 $\pm$ 1.08
131-62	99.50	99.48	0.129580 $\pm$ 0.000041	0.0772060 $\pm$ 0.000023	0.153978 $\pm$ 0.000048	90	24.84 $\pm$ 2.48	64	3.11 $\pm$ 1.93	92 12.77 $\pm$ 1.83
Hugo Microcline										
PMO 147-57			0.129749 $\pm$ 0.000042	0.077216 $\pm$ 0.000016	0.154137 $\pm$ 0.000033	90	23.25 $\pm$ 1.81	64	3.46 $\pm$ 1.11	92 11.73 $\pm$ 1.23
Hugo Albite										
PMO 143-47			0.137458 $\pm$ 0.000018	0.078454 $\pm$ 0.000012	0.156593 $\pm$ 0.000016	86	24.42 $\pm$ 1.02	63	28.19 $\pm$ 0.67	90 27.24 $\pm$ 0.87
Hugo Albite (KCl Exchange)			0.129659 $\pm$ 0.000033	0.077200 $\pm$ 0.000017	0.153965 $\pm$ 0.000031	90	25.64 $\pm$ 1.44	64	4.70 $\pm$ 1.08	92 16.36 $\pm$ 1.40

subprogram. Results of this refinement are given in Tables 2 and 3 and are plotted in Figures 3, 4, and 5. Standard errors were also calculated by this computer program and they give some indication of the internal consistency of the measured  $2\theta$  values. Where the standard error in a unit-cell parameter is greater than the radius of the circle used on the diagram to plot data points, its magnitude is indicated by a vertical bar of appropriate length.

TABLE 2C. CALCULATED SPACINGS OF SELECTED PLANES, MICROCLINE-LOW ALBITE SERIES

Composition			$d(\bar{2}01)$ Å	$d(400)$ Å	$d(060)$ Å	$d(\bar{2}04)$ Å	$d(\bar{1}\bar{3}1)$ Å	$d(131)$ Å
Sample	wt% Or	mole% Or						
128-62	1.00	0.94	4.0306	1.8188	2.1247	1.7842	2.9614	2.8608
55-63	10.85	10.27	4.0473	1.8296	2.1280	1.7865	2.9621	2.8780
157-63	20.70	19.71	4.0695	1.8438	2.1371	1.7909	2.9621	2.9093
49-63	30.55	29.27	4.0950	1.8545	2.1447	1.7953	2.9600	2.9306
51-63	40.40	38.96	4.1158	1.8711	2.1490	1.7982	2.9519	2.9671
158-63	50.25	48.76	4.1345	1.8818	2.1519	1.7997	2.9512	2.9856
57-63	60.10	58.68	4.1513	1.8913	2.1538	1.8009	2.9492	2.0008
50-63	69.95	68.71	4.1744	1.9034	2.1565	1.8027	2.9507	3.0140
156-63	79.80	78.86	4.1910	1.9128	2.1574	1.8032	2.9527	3.0222
56-63	89.65	89.11	4.2082	1.9204	2.1575	1.8036	2.9532	3.0260
131-62	99.50	99.48	4.2276	1.9293	2.1587	1.8053	2.9560	3.0320
Hugo Microcline PMO 147-57			4.2222	1.9289	2.1584	1.8046	2.9553	3.0299
Hugo Albite PMO 143-57			4.0278	1.8187	2.1244	1.7843	2.9626	2.8613
Hugo Albite (KCl Exchange)			4.2241	1.9281	2.1589	1.8051	2.9550	3.0332

The curves plotted in Figures 3, 4 and 5 are computer calculated least square polynomial regressions of the unit-cell parameters with composition as calculated by the U. S. Geological Survey's computer. The equations of the curves are given in Table 4. Regression curves of third, second and first order were calculated but the lowest order curve that gives a good representation of the data has been used. All curves are third order except those representing  $a$ ,  $b$  and  $\gamma$  for the microcline-low albite series and  $\alpha$  for the sanidine-high albite series which are second order.

Tables listing intensity, quality, index and position of all observed X-ray peaks and the computer output for the final unit-cell refinement for each feldspar sample have been deposited as Document No. 9225

TABLE 3A. DIRECT UNIT-CELL PARAMETERS, SANDINE-HIGH ALBITE SERIES

Composition		No. Lines	a Å	b Å	c Å	$\alpha$ deg. min.	$\beta$ deg. min.	$\gamma$ deg. min.	Volume	
Wt% Or	Mole% Or								Å <sup>3</sup>	cm <sup>3</sup> /mol
0.00	0.00	20	8.1506±0.0024	12.8616±0.0020	7.1151±0.0010	93.39.01±1.12	116.27.07±1.20	89.59.09±0.97	666.11±0.18	100.29
5.00	4.72	21	8.1665±0.0027	12.8738±0.0020	7.1175±0.0009	93.22.53±0.94	116.27.58±1.16	90.7.31±0.94	668.42±0.19	100.64
10.00	9.47	21	8.1988±0.0028	12.8883±0.0027	7.1234±0.0013	92.59.42±1.39	116.26.63±1.62	90.14.08±1.51	672.73±0.22	101.29
15.00	14.26	18	8.2129±0.0033	12.9096±0.0031	7.1320±0.0014	92.42.61±1.66	116.24.44±1.83	90.11.60±2.31	676.27±0.27	101.82
20.00	19.06	19	8.2347±0.0032	12.9245±0.0020	7.1368±0.0010	92.17.26±1.25	116.23.69±1.26	90.12.72±1.38	679.65±0.23	102.33
25.00	23.90	16	8.2526±0.0028	12.9351±0.0019	7.1431±0.0008	91.55.63±1.02	116.20.36±1.04	90.8.47±1.39	682.84±0.21	102.81
30.00	28.76	17	8.2820±0.0045	12.9541±0.0032	7.1489±0.0014	91.25.53±1.61	116.19.35±1.72	80.8.69±1.94	687.16±0.35	103.46
35.00	33.66	17	8.2893±0.0036	12.9593±0.0041	7.1537±0.0020	90.45.33±2.27	116.17.25±2.08	89.57.12±2.60	688.94±0.34	103.73
40.00	38.58	23	8.3205±0.0012	12.9771±0.0017	7.1585±0.0009	90.00.00±0.84	116.11.75±0.93	90.00±0.78	693.56±0.15	104.42
45.00	43.53	15	8.3479±0.0015	12.9849±0.0016	7.1637±0.0009	90.00	116.9.53±1.13	90.00	696.99±0.17	104.94
50.00	48.51	16	8.3752±0.0013	12.9895±0.0017	7.1646±0.0009	90.00	116.8.62±1.15	90.00	699.69±0.16	105.35
55.00	53.52	16	8.4017±0.0024	12.9936±0.0021	7.1643±0.0010	90.00	116.7.44±1.47	90.00	702.22±0.21	105.73
60.00	58.56	15	8.4250±0.0020	12.9988±0.0017	7.1668±0.0009	90.00	116.5.66±1.24	90.00	704.87±0.18	106.13
65.00	63.63	22	8.4487±0.0010	13.0128±0.0013	7.1701±0.0006	90.00	116.2.35±0.521	90.00	708.28±0.09	106.64
70.00	68.73	24	8.4705±0.0007	13.0111±0.0010	7.1711±0.0005	90.00	116.1.85±0.412	90.00	710.15±0.07	106.92
75.00	73.87	26	8.4970±0.0008	13.0148±0.0011	7.1714±0.0006	90.00	116.707±0.477	90.00	712.73±0.08	107.31
80.00	79.03									
85.00	84.22	26	8.5447±0.0011	13.0206±0.0013	7.1759±0.0007	90.00	116.1.259±0.558	90.00	717.45±0.10	108.02
90.00	89.45	29	8.5582±0.0008	13.0196±0.0010	7.1769±0.0006	90.00	116.026±0.428	90.00	718.76±0.08	108.22
95.00	94.71	28	8.5851±0.0009	13.0273±0.0012	7.1788±0.0007	90.00	116.86±0.502	90.00	721.54±0.09	108.64
100.00	100.00	26	8.6027±0.0008	13.0209±0.0010	7.1777±0.0005	90.00	116.62±0.434	90.00	722.57±0.08	108.79

TABLE 3B. RECIPROCAL UNIT-CELL PARAMETERS, SANDINE-HIGH ALBITE SERIES

Composition		$a^*$		$b^*$		$c^*$		$\alpha^*$		$\beta^*$		$\alpha^*$	
wt% Of	mole% Or	$1/\text{\AA}$		$1/\text{\AA}$		$1/\text{\AA}$		deg. min		deg. min		deg. min	
0.00	0.00	0.137104 $\pm$ 0.000039	0.077947 $\pm$ 0.000012	0.157376 $\pm$ 0.000029	85 55 79 $\pm$ 1.27	63 29.52 $\pm$ 1.20	88 11.89 $\pm$ 0.90						
5.00	4.72	0.136847 $\pm$ 0.000045	0.077851 $\pm$ 0.000012	.157289 $\pm$ .000027	86 10.09 $\pm$ 0.93	63 28.96 $\pm$ 1.16	88 10.88 $\pm$ 0.91						
10.00	9.47	0.136285 $\pm$ 0.000039	0.077737 $\pm$ 0.000016	.157073 $\pm$ .000038	86 32.58 $\pm$ 1.27	63 30.21 $\pm$ 1.64	88 14.92 $\pm$ 1.41						
15.00	14.26	0.135995 $\pm$ 0.000046	0.077577 $\pm$ 0.000019	.156780 $\pm$ .000042	86 52.66 $\pm$ 1.43	63 33.02 $\pm$ 1.84	88 26.21 $\pm$ 2.15						
20.00	19.06	0.135609 $\pm$ 0.000048	0.077450 $\pm$ 0.000012	.156595 $\pm$ .000027	87 20.44 $\pm$ 1.06	63 34.37 $\pm$ 1.26	88 37.26 $\pm$ 1.20						
25.00	23.90	0.135237 $\pm$ 0.000042	0.077367 $\pm$ 0.000011	.156330 $\pm$ .000024	87 46.75 $\pm$ 1.00	63 38.35 $\pm$ 1.05	88 53.26 $\pm$ 1.38						
30.00	28.76	0.134726 $\pm$ 0.000070	0.077228 $\pm$ 0.000019	.156130 $\pm$ .000040	88 20.27 $\pm$ 1.69	63 39.88 $\pm$ 1.72	89 7.98 $\pm$ 2.01						
35.00	33.66	0.134554 $\pm$ 0.000066	0.077172 $\pm$ 0.000024	.155928 $\pm$ .000050	89 10.86 $\pm$ 2.09	63 42.65 $\pm$ 2.09	89 40.82 $\pm$ 2.46						
40.00	38.58	0.133941 $\pm$ 0.000043	0.077059 $\pm$ 0.000010	.155683 $\pm$ .000023	90 0 00 $\pm$ 0.93	63 48.25 $\pm$ 0.93	90 0 00 $\pm$ 0.87						
45.00	43.53	0.133460 $\pm$ 0.000034	0.077012 $\pm$ 0.000010	.155522 $\pm$ .000026	90	63 50.47 $\pm$ 1.13	90						
50.00	48.51	0.133009 $\pm$ 0.000032	0.076985 $\pm$ 0.000010	.155482 $\pm$ .000026	90	63 51.38 $\pm$ 1.15	90						
55.00	53.52	0.132565 $\pm$ 0.000042	0.076961 $\pm$ 0.000012	.155463 $\pm$ .000030	90	63 52.57 $\pm$ 1.47	90						
60.00	58.56	0.132166 $\pm$ 0.000036	0.076930 $\pm$ 0.000010	.155369 $\pm$ .000027	90	63 54.34 $\pm$ 1.24	90						
65.00	63.63	0.131733 $\pm$ 0.000016	0.076847 $\pm$ 0.000008	.155223 $\pm$ .000013	90	63 57.65 $\pm$ 0.52	90						
70.00	68.73	0.131385 $\pm$ 0.000011	0.076858 $\pm$ 0.000006	.155191 $\pm$ .000010	90	63 58.15 $\pm$ 0.41	90						
75.00	73.87	0.130954 $\pm$ 0.000012	0.076835 $\pm$ 0.000007	.155159 $\pm$ .000012	90	63 59.29 $\pm$ 0.48	90						
80.00	79.03												
85.00	84.22	0.130233 $\pm$ 0.000016	0.076801 $\pm$ 0.000008	.155074 $\pm$ .000015	90	63 58.75 $\pm$ 0.56	90						
90.00	89.45	0.130004 $\pm$ 0.000012	0.076807 $\pm$ 0.000006	.155025 $\pm$ .000012	90	63 59.98 $\pm$ 0.43	90						
95.00	94.71	0.129612 $\pm$ 0.000014	0.076762 $\pm$ 0.000007	.155004 $\pm$ .000015	90	63 59.14 $\pm$ 0.50	90						
100.00	100.00	0.129344 $\pm$ 0.000012	0.076800 $\pm$ 0.000006	.155022 $\pm$ .000012	90	63 59.39 $\pm$ 0.43	90						

TABLE 3C. CALCULATED SPACINGS OF SELECTED PLANES,  
SANIDINE-HIGH ALBITE SERIES

Composition		$d(201)$	$d(400)$	$d(060)$	$d(204)$	$d(1\bar{3}1)$	$d(131)$
wt% Or	mole% Or	Å	Å	Å	Å	Å	Å
0.00	0.00	4.0345	1.8235	2.1382	1.7750	3.0115	2.8313
5.00	4.72	4.0420	1.8260	2.1408	1.7762	3.0111	2.8378
10.00	9.47	4.0567	1.8344	2.1441	1.7782	3.0101	2.8503
15.00	14.26	4.0632	1.8383	2.1484	1.7809	3.0079	2.8638
20.00	19.06	4.0731	1.8436	2.1518	1.7826	3.0026	2.8784
25.00	23.90	4.0809	1.8487	2.1542	1.7846	2.9999	2.8939
30.00	28.76	4.0943	1.8556	2.1581	1.7865	2.9904	2.9122
35.00	33.90	4.0974	1.8618	2.1597	1.7881	2.9717	2.9363
40.00	38.58	4.1107	1.8666	2.1628	1.7895	2.9614	2.9614
45.00	43.53	4.1228	1.8732	2.1642	1.7908	2.9659	
50.00	48.51	4.1348	1.8796	2.1649	1.7910	2.9692	
55.00	53.52	4.1464	1.8859	2.1656	1.7908	2.9722	
60.00	58.56	4.1565	1.8919	2.1665	1.7915	2.9757	
65.00	63.63	4.1666	1.8979	2.1688	1.7923	2.9808	
70.00	68.73	4.1761	1.9028	2.1685	1.7925	2.9827	
75.00	73.87	4.1876	1.9091	2.1691	1.7926	2.9857	
80.00	79.03						
85.00	84.22	4.2089	1.9198	2.1701	1.7936	2.9906	
90.00	89.45	4.2146	1.9230	2.1699	1.7938	2.9921	
95.00	94.71	4.2266	1.9298	2.1712	1.7942	2.9950	
100.00	100.00	4.234	1.9330	2.1702	1.7939	2.9957	

with the ADI, Auxiliary Publications Project, Photoduplication Service, Library of Congress, Washington 25, D. C.<sup>1</sup>

## RESULTS

*Unit-cell dimension a.* From Figure 3 it can be seen that  $a$  varies strongly with composition and is only slightly dependent on Al:Si ordering. Where precise unit cell data are available, the length of  $a$  provides a reliable and sensitive indicator of composition for homogeneous or coarsely perthitic alkali feldspar phases.<sup>2</sup> The greatest separation between the microcline-

<sup>1</sup> Copies may be secured by citing the Document number, and remitting in advance \$10.00 for photoprints or \$3.50 for microfilm, payable to Chief, Photoduplication Service, Library of Congress.

<sup>2</sup> Laves (1952b) and Smith (1961) have pointed out that the unit cell dimensions of exsolved phases in cryptoperthitic feldspars are distorted from those of homogeneous or coarsely perthitic exsolved phases of the same compositions. Therefore an X-ray determinative curve based upon homogeneous unstrained alkali feldspars will not generally be valid for the phases of cryptoperthites.

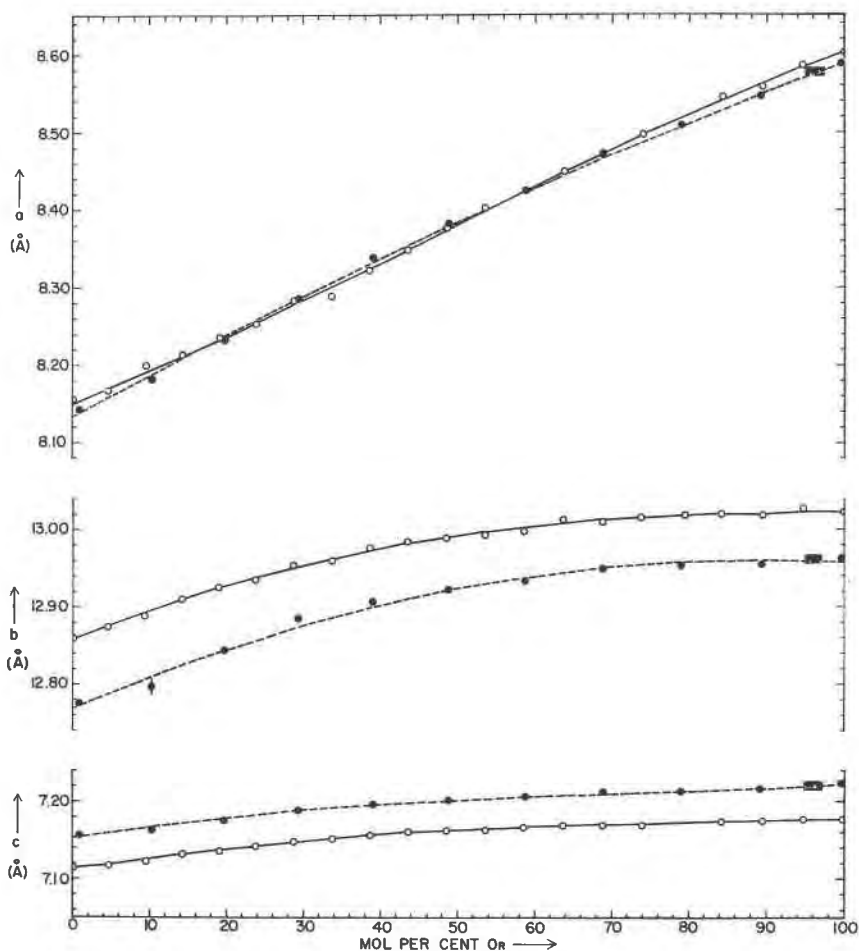


FIG. 3. Unit-cell dimensions  $a$ ,  $b$  and  $c$ . Radius of data point circles is equivalent to .002 Å; larger standard errors indicated by a vertical line. Open circles and solid curve represent sanidine-high albite solid solution. Closed circles and dashed curve represent microcline-low albite solid solutions. Closed rectangle represents Hugo microcline starting material. Equations for regression curves given in Table 4.

low albite and the sanidine-high albite curves is equivalent to about 4 percent difference in Or-content. The effect of Al:Si state is therefore not trivial since  $a$  can be determined to better than  $\pm 0.004$  Å, the equivalent of  $\pm 1$  percent Or.

*Unit-cell dimensions b and c.* The  $b$  and  $c$  unit-cell dimensions depend upon both composition and Al:Si order. The change from a more ordered to a

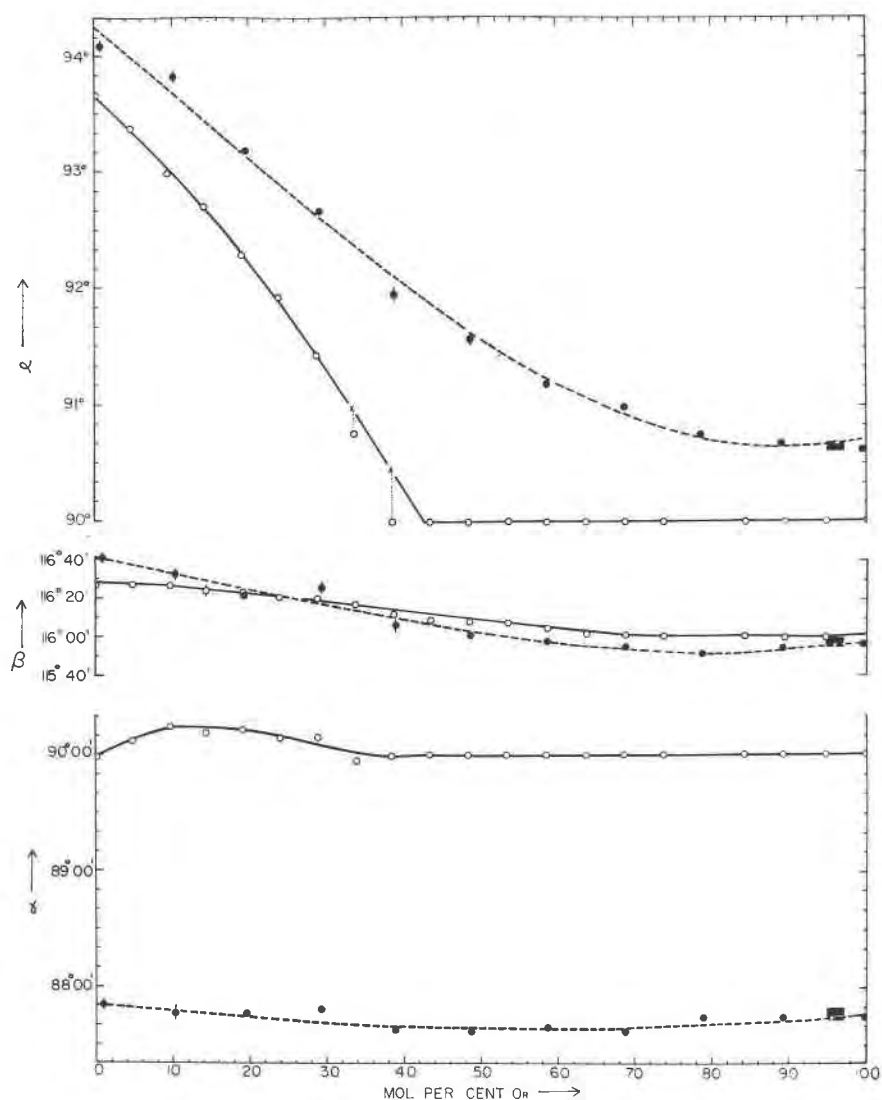


FIG. 4. Unit-cell angles. Radius of data point circles is equivalent to  $2\sigma$ ; larger standard errors indicated by vertical line. Open circles and solid curve represent sandine-high albite solid solution. Closed circles and dashed curve represent microcline-low albite solid solution. Closed rectangle represents Hugo microcline starting material. Equations for regression curves given in Table 4.

Values of  $\alpha$  for sandine-high albite solid solution compositions  $Or_{33.7}$  and  $Or_{38.6}$  (mole percent) are known to be in error because of mutual interference of X-ray peaks belonging to pairs of the type  $(hkl)-(h\bar{k}l)$ . The regression curve for  $\alpha$  has been fitted for compositions in the range  $Or_{0.0}$ - $Or_{28.8}$  (mole percent). Extrapolation of this curve to higher Or-contents is thought to provide the best estimate of  $\alpha$  for sandine-high albite solid solution compositions between  $Or_{28.8}$  and the triclinic-monoclinic transition.

less ordered structural state produces an increase in  $b$  and decrease in  $c$ . Cole, Sørum and Kennard (1949) first observed this for the transition orthoclase-sanidine and showed that disordering of Al and Si between the  $T_1$  and  $T_2$  positions can be expected to have this effect. These unit-cell parameters provide a description of Al:Si order independent of symmetry and are therefore applicable to monoclinic as well as triclinic alkali feldspars. Stewart (written communication) and Wright (1964) have shown

TABLE 4. LEAST SQUARES POLYNOMIAL REGRESSION OF ALKALI FELDSPAR UNIT-CELL PARAMETERS (Y) WITH COMPOSITION (X=MOLE PERCENT OR)

Y =	A+B	X+C	X <sup>2</sup> +D	X <sup>3</sup> Standard Error
<b>Sanidine-High Albite Series</b>				
$a$ (Å) =	$8.15328 + 3.6749 \times 10^{-3} X$	$X + 2.6874 \times 10^{-5}$	$X^2 - 1.8688 \times 10^{-7}$	$X^{30.0048}$ Å
$b$ (Å) =	$12.85722 + 4.0877 \times 10^{-3} X$	$X - 3.1560 \times 10^{-5}$	$X^2 + 7.217 \times 10^{-8}$	$X^{30.0035}$ Å
$c$ (Å) =	$7.11150 + 1.6805 \times 10^{-3} X$	$X - 1.5067 \times 10^{-5}$	$X^2 + 4.937 \times 10^{-8}$	$X^{30.0018}$ Å
$\alpha^{92} = 93^\circ$	$38.82 - 3.50832 X$	$X - 0.037707$	$X^2$	$1.9'$
$\beta = 116^\circ$	$28.37' - 0.1896' X$	$X - 7.529 \times 10^{-3}$	$X^2 + 6.782 \times 10^{-5}$	$X^{21.1}'$
$\gamma^{89} = 89^\circ$	$58.96' + 2.4048' X$	$X - 0.116174$	$X^2 + 1.38964 \times 10^{-3}$	$X^{32.8}'$
$V$ (Å <sup>3</sup> ) =	$665.511 + 0.76768 X$	$X - 9.460 \times 10^{-4}$	$X^2 - 1.0227 \times 10^{-5}$	$X^{30.52}$ Å <sup>3</sup>
$V_{\text{mix}}$ (Å <sup>3</sup> ) =	$0.19687$	$X - 9.460 \times 10^{-4}$	$X^2 - 1.0227 \times 10^{-5}$	$X^{30.65}$ Å <sup>3</sup>
<b>Microcline-Low Albite Series</b>				
$a$ (Å) =	$8.13085 + 4.5497 \times 10^{-3} X$	$X - 9.596 \times 10^{-6}$	$X^2$	$0.0046$ Å
$b$ (Å) =	$12.77009 + 4.3049 \times 10^{-3} X$	$X - 2.4395 \times 10^{-5}$	$X^2$	$0.0079$ Å
$c$ (Å) =	$7.15111 + 1.5865 \times 10^{-3} X$	$X - 1.3699 \times 10^{-5}$	$X^2 + 4.872 \times 10^{-8}$	$X^{30.0027}$ Å
$\alpha = 94^\circ$	$15.03' - 3.3775' X$	$X - 5.572 \times 10^{-3}$	$X^2 + 1.7955 \times 10^{-4}$	$X^{36.6}'$
$\beta = 116^\circ$	$41.02' - 0.7554' X$	$X - 4.001 \times 10^{-3}$	$X^2 + 7.297 \times 10^{-5}$	$X^{33.9}'$
$\gamma = 87^\circ$	$51.92' - 0.4336' X$	$X + 3.759 \times 10^{-3}$	$X^2$	$3.2'$
$V$ (Å <sup>3</sup> ) =	$661.628 + 0.94301 X$	$X - 3.1804 \times 10^{-3}$	$X^2 - 2.149 \times 10^{-6}$	$X^{31.03}$ Å <sup>3</sup>
$V_{\text{mix}}$ (Å <sup>3</sup> ) =	$0.33953$	$X - 3.1804 \times 10^{-3}$	$X^2 - 2.149 \times 10^{-6}$	$X^{31.30}$ Å <sup>3</sup>

<sup>1</sup> Equation applies only to triclinic members of sanidine-high albite solid solution.

<sup>2</sup> Equation fitted to data for composition range Or<sub>0</sub>-Or<sub>28.8</sub> mole percent.

the usefulness of  $b$ - $c$  plots in classifying alkali feldspar solid solutions. (See also Fig. 11.)

**Unit-cell angles.** In monoclinic alkali feldspars both  $\alpha$  and  $\gamma$  are fixed at  $90^\circ$ . For triclinic alkali feldspars,  $\alpha$  is sensitive to composition and rather insensitive to Al:Si order whereas  $\gamma$  shows a pronounced change with Al:Si order and is almost independent of composition. The value of  $\beta$  varies so little that it is not useful for characterizing the alkali feldspar solid solution.

**Volume.** The unit-cell volume curves (Fig. 5) for the microcline-low albite and the sanidine-high albite series nearly coincide between Or<sub>100</sub> and Or<sub>20</sub>Ab<sub>80</sub>. More Ab-rich compositions show significantly lower volumes for the microcline-low albite series, and at Ab<sub>100</sub> the difference is  $3.8 \pm 1.1$



$\text{\AA}^3$  (corresponding to  $0.57 \pm 0.17 \text{ cm}^3/\text{mole}$ ). This implies that confining pressure can have very little effect on the Al:Si ordering of K-rich feldspars but that ordering of Ab-rich feldspars will be aided by high confining pressure.

The effect of pressure on the low albite-high albite transition can be

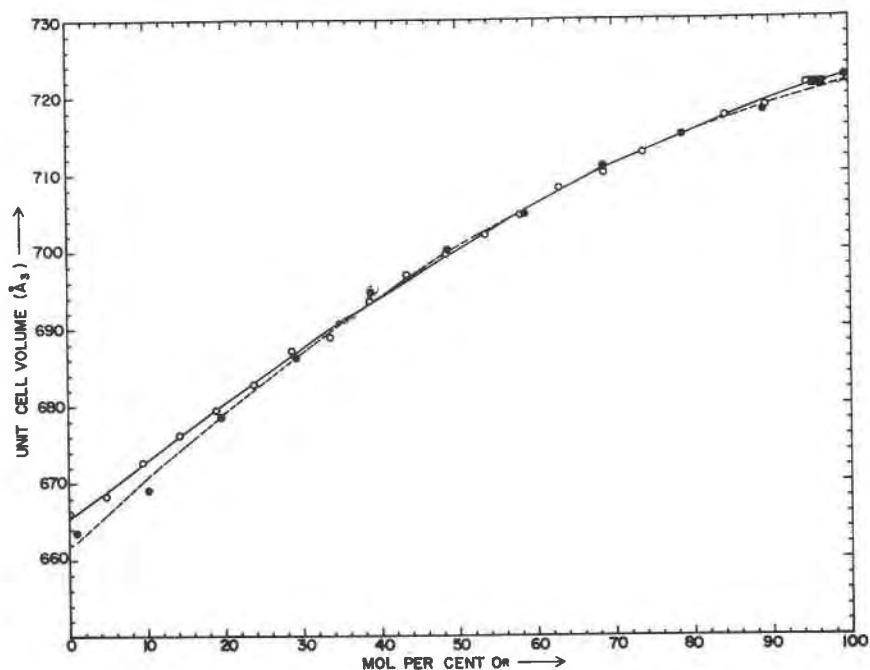


FIG. 5. Unit-cell volume. Radius of data point circles is equivalent to  $0.5 \text{ \AA}^3$ . Open circles and solid curve represent sanidine-high albite solid solution. Closed circles and dashed curve represents microcline-low albite solid solution. Closed rectangle represents Hugo Microcline starting material. Equations for regression curves given in Table 4.

calculated if it is assumed that it is a first order transition or the major part of the ordering takes place over a limited range of temperature. The entropy change for the transition will be largely due to disordering one Al and three Si cations over four tetrahedral sites which is

$$S = R(1/4 \ln 1/4 + 3/4 \ln 3/4) = 1.12 \text{ cal deg}^{-1} \text{ mole}^{-1}$$

$$= 47.0 \text{ cm}^3 \text{ bar deg}^{-1} \text{ mole}^{-1}$$

(Fyfe, Turner and Verhoogen, 1958, p. 32).

The effect of pressure on the transition temperature can be calculated from the Clausius-Clapeyron equation

$$\frac{dP}{dT} (\text{low Ab} \rightarrow \text{high Ab}) = \frac{\Delta S}{\Delta V} = 83 \pm 25 \text{ bar deg}$$

An increase of 1000 bars in confining pressure should therefore raise the low albite-high albite transition by 9 to 17°C.

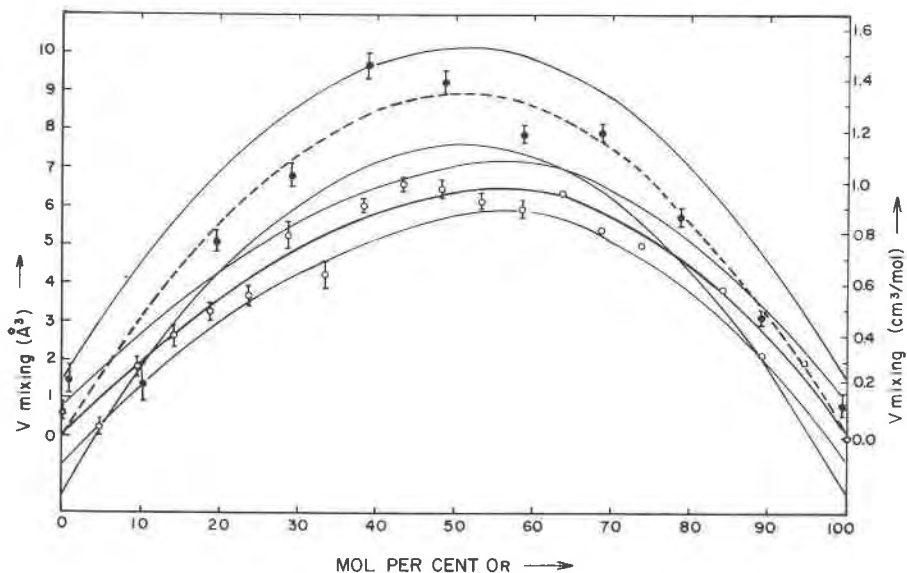


FIG. 6. Volume of mixing. Difference between observed volume and linear extrapolation of volume between  $\text{Or}_0$  and  $\text{Or}_{100}$ . Radius of data point circles is equivalent to  $0.1 \text{ \AA}^3$ . Larger standard errors indicated by vertical line. Open circles and solid curve represent sanidine-high albite solid solution. Closed circles and dashed curve represents microcline-low albite solid solution. Equations for regression curves are given in Table 4.

The volume curves for both feldspar solid solutions show positive volumes of mixing. Volume of mixing is plotted in Figure 6 and the equations for the regression curves are given in Table 4. The maximum volume of mixing for the microcline-low albite solid solution is  $8.8 \pm 1.3 \text{ \AA}^3$  ( $1.30 \pm 0.19 \text{ cm}^3 \text{ mole}^{-1}$  or  $1.25 \pm 0.18\%$ ) at  $\text{Or}_{50.6}$  mole percent and the maximum for the sanidine-high albite solid solution is  $6.3 \pm 0.6 \text{ \AA}^3$  ( $0.94 \pm 0.09 \text{ cm}^3 \text{ mole}^{-1}$  or  $0.90 \pm 0.09\%$ ) at  $\text{Or}_{55.1}$  mole percent. Uncertainty in the position of the maximum is estimated to be on the order of  $\pm 10$  mole percent for both

curves. Both curves are so close to parabolas that the volume of mixing can probably be adequately represented by second order equations.

The volume of mixing relations shown here requires that the solvus crest must increase in temperature and the solid solution gap increase in width with increasing pressure for both feldspar solid solutions; the change in the microcline-low albite solvus being greater than that for the sanidine-high albite solvus. Furthermore, the crest of the sanidine-high albite solvus, located at  $\text{Or}_{30} \pm 10$  mole percent at 2000 bars pressure

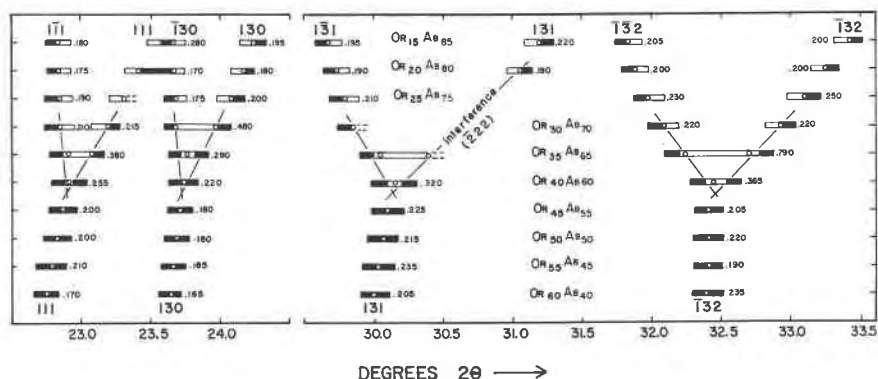


FIG. 7. Pairs of sanidine-high albite X-ray diffraction peaks in vicinity of triclinic-monoclinic transition. Open circles represent peak maxima. Feldspar compositions given in weight percent. Width of peaks measured at half peak height indicated by horizontal bar and numerical value in degrees  $2\theta$  for  $\text{CuK}\alpha$  radiation. "Excess width" for peaks of  $\text{Or}_{35}\text{Ab}_{65}$  and  $\text{Or}_{40}\text{Ab}_{60}$  compositions represented by open bars. Straight line extrapolation of peak separations at  $\text{Or}_{30}\text{Ab}_{70}$  through "excess width" at  $\text{Or}_{40}\text{Ab}_{60}$  composition indicates minimum Or-content at triclinic-monoclinic transition.

(Orville, 1963), must move to more Or-rich compositions with increasing pressure.

*Symmetry change in the sanidine-high albite solid solution.* Donnay and Donnay (1952) concluded that the change from monoclinic to triclinic symmetry at room temperature for the synthetic high temperature alkali feldspar series occurs at slightly less than 35 wt percent Or molecule. X-ray powder patterns of  $\text{Or}_{35}\text{Ab}_{65}$  synthesized in this study show definite splitting and broadening of peaks that should be single sharp peaks if the symmetry were truly monoclinic and patterns of  $\text{Or}_{40}\text{Ab}_{60}$  also show some broadening of certain peaks.

Four representative pairs of peaks that become a single peak at the transition have been plotted in Figure 7 over a range of composition that

includes the transition. The observed midpoint of the top of each peak is shown together with the width measured at half the peak height. The latter is also given a numerical value in degrees  $2\theta$ . At  $\text{Or}_{40}\text{Ab}_{60}$  composition, each pair of peaks shown in Figure 7 has become an apparently single peak. The widths, however, are significantly larger than widths measured for single peaks and this "excess width" has been indicated graphically for  $\text{Or}_{35}\text{Ab}_{65}$  and  $\text{Or}_{40}\text{Ab}_{60}$  compositions in Figure 7. The "excess width" of a doublet peak will be somewhat less than the spacing of the doublet. Linear extrapolation from  $\text{Or}_{30}\text{Ab}_{70}$  composition peaks through the "excess width" at  $\text{Or}_{40}\text{Ab}_{60}$  composition therefore indicates that the triclinic-monoclinic transition is at least as Or-rich as  $\text{Or}_{42}\text{Ab}_{58}$ . The widths of peaks for  $\text{Or}_{45}\text{Ab}_{55}$  composition are normal for single peaks. On this basis the best estimate for the transition from triclinic to monoclinic symmetry at room temperature is at  $\text{Or}_{43.5}\text{Ab}_{56.5} \pm 2.0$  weight percent or  $\text{Or}_{42.0} \pm 2.0$  mole percent. Extrapolation of  $\alpha$  by the second degree regression equation given in Table 4 locates the triclinic-monoclinic symmetry transition at  $\text{Or}_{42.0} \pm 0.3$  mole percent, well within the limits given above.

#### DISCUSSIONS AND APPLICATIONS

*X-ray determinative curves for alkali feldspars.* Although present-day computer techniques have made it possible to determine unit cell parameters from X-ray powder patterns almost as a matter of routine, it is not always practical or possible to determine the  $a$  unit cell dimension for every feldspar sample.

A new X-ray determinative curve for the microcline-low albite series utilizing the  $\bar{2}01$  reflection is shown in Figure 8. Composition of the feldspar (in mole percent Or) is plotted directly against  $\Delta 2\theta$ , the difference in  $2\theta$  between the  $\bar{2}01$  reflection of alkali feldspar and the  $(101)$  reflection of  $\text{KBrO}_3$  for  $\text{CuK}\alpha_1$  radiation. Each of the eleven points in Figure 8 represents an average of 12 measurements of  $\Delta 2\theta$ . Two straight lines that intersect at  $\text{Or}_{45}$  fit the data points very well. These lines have  $\Delta 2\theta$  values of .765, 1.280 and 1.850 degrees at compositions of  $\text{Or}_{100}$ ,  $\text{Or}_{45}$   $\text{Or}_0$ , respectively. The Or-rich portion of this curve is essentially identical with the microcline determinative curve of Orville (1960). The determinative curve for the sanidine-high albite series (Orville, 1963) is shown as a solid line for comparison.

X-ray determinative curves for the alkali feldspars have been based upon the  $\bar{2}01$  reflection (Bowen and Tuttle, 1950; Orville, 1959, 1963, and this paper) and upon the  $(400)$  reflection (Goldsmith and Laves, 1961). Calculated values of  $d(400)$  and  $d(\bar{2}01)$  are given for the sanidine-high albite series in Table 2 and the microcline-low albite series in Table 3.

These values are plotted for both alkali feldspar series in Figure 9. The microcline-low albite curve of Goldsmith and Laves (1961) and of Orville (this paper) and the sanidine-high albite curves of Orville (1963) and Bowen and Tuttle (1950) are shown for comparison. The  $\Delta 2\theta$  curves based on a  $\text{KBrO}_3$  internal standard have been converted to  $d(201)$  by calibration of the (101) reflection of  $\text{KBrO}_3$  against the (110) reflection

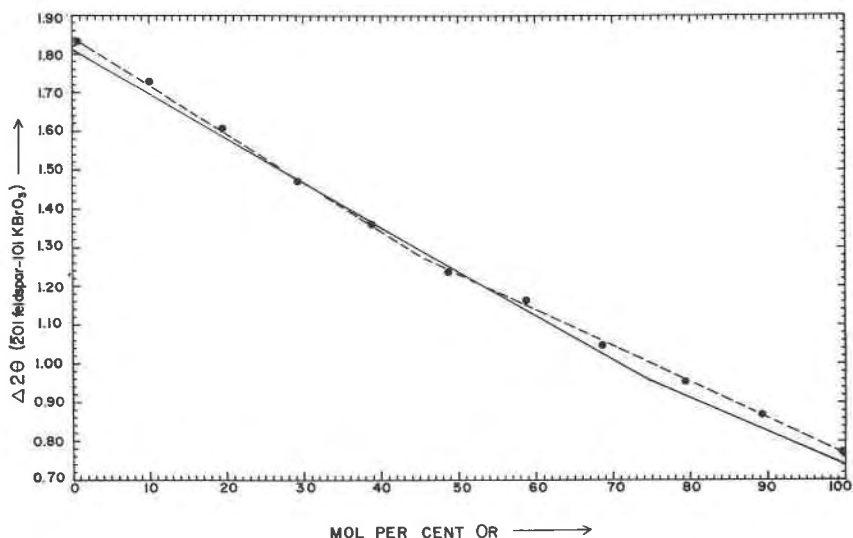


FIG. 8.  $\Delta 2\theta$  curve for microcline-low albite solid solution.  $\Delta 2\theta = 2\theta(201)$  feldspar  $- 2\theta(101)\text{KBrO}_3$  for  $\text{CuK}\alpha$  radiation. Solid circles and dashed line represent microcline-low albite solid solution. Microcline-low albite determinative curve consists of two straight line segments that intersect at  $\text{Or}_{45}$  mole percent. These lines have  $\Delta 2\theta = .765, 1.280$  and  $1.850$  at compositions  $\text{Or}_{100}, \text{Or}_{45}$  and  $\text{Or}_0$ , respectively. For conversion to absolute  $2\theta$  values for  $\text{CuK}\alpha$ , radiation, add  $20.212^\circ$  to each  $\Delta 2\theta$  value. The sanidine-high albite determinative curve of Orville, 1963, is shown as a solid line.

of  $\text{CaF}_2$ . This calibration makes  $d(101)\text{KBrO}_3$  equal to  $4.3896 \text{ \AA}$  and  $2\theta(101)\text{KBrO}_3$  equal to  $20.212^\circ$  for  $\text{CuK}\alpha_1$  radiation.

As a check on the applicability of the 201 determinative curves to natural alkali feldspars,  $\Delta 2\theta$  values were determined for chemically analyzed microcline perthite specimens that had been homogenized by both hydrothermal treatment and by dry heating. The hydrothermal treatment at  $800^\circ\text{C}$  and 1000 bars  $\text{H}_2\text{O}$  pressure for 21 days produced a homogeneous monoclinic feldspar phase and dry heating at  $1050^\circ\text{C}$  for 48 hours resulted in a homogeneous triclinic feldspar phase. These data are plotted in Figure 10 together with the relevant portions of the micro-

cline-low albite and sanidine-high albite determinative curves. There is a systematic difference in  $\Delta 2\theta$  values between the dry and hydrothermal homogenized perthite that is consistent with the difference found in the positions of the microcline-low albite and sanidine-high albite determinative curves. From these results it appears that a composition error of up

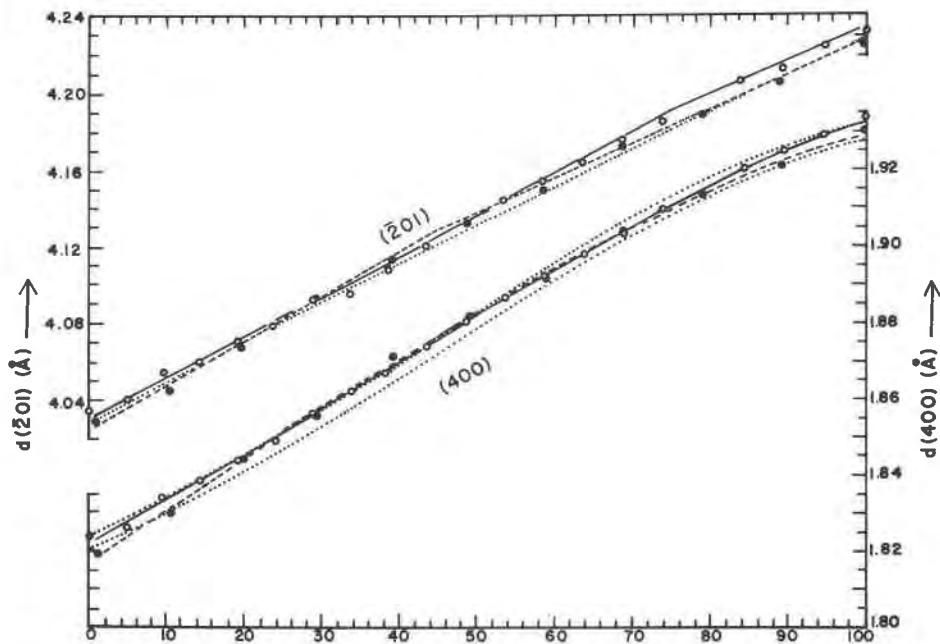


FIG. 9. Calculated  $d(201)$  and  $d(400)$  for microcline-low albite and sanidine-high albite solid solutions. Open circles and solid lines represent sanidine-high albite solid solution. Closed circles and dashed lines represent microcline-low albite solid solution. Dotted lines for (400) are curves of Goldsmith and Laves (1961) (upper curve sanidine-high albite solid solution, lower curve microcline-low albite solid solution). Dotted line for (201) is sanidine-high albite curve of Bowen and Tuttle (1950).

to 3 percent (Or) may be introduced into a  $\overline{201}$  feldspar determination solely through use of a determinative curve for an inappropriate structural state.

#### STRUCTURAL STATES OF ALKALI FELDSPARS

Alkali feldspars of the sanidine-high albite series, the microcline-low albite series and the Hugo microcline, Hugo albite and KCl-exchanged Hugo albite are plotted on a  $b$ - $c$  diagram in Figure 11 and a  $\alpha$ - $\gamma$  diagram in Figure 12. Both types of plot clearly separate the two feldspar



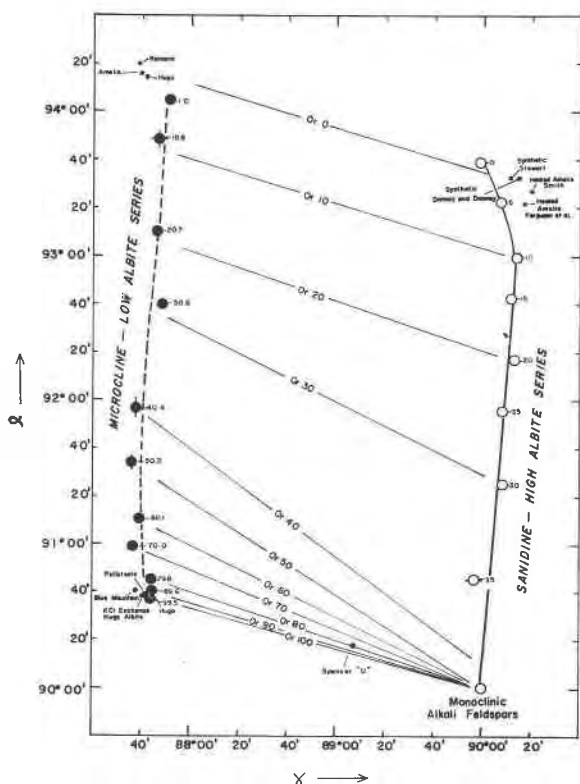


FIG. 12. Unit-cell dimensions  $\alpha$ - $\gamma$  plot. Microcline-low albite and sanidine-high albite solid solutions from Tables 2 and 3; other alkali feldspars from Tables 5 and 6. Compositions of microcline-low albite and sanidine-high albite solid solutions given in weight percent. Constant composition tie lines drawn between high and low series.

series. Several Ab-rich and Or-rich alkali feldspars described by other authors are also plotted and unit-cell data and references for these feldspars are given in Tables 5 and 6.

*Sanidine-high albite series.* The Ab-rich end of the sanidine-high albite series falls toward more ordered structures than those represented by the high albites of Smith (1956), Stewart and Von Limbach (1967) and Ferguson, Traill and Taylor (1958) on both the  $b$ - $c$  and  $\alpha$ - $\gamma$  plots. The differences are not too surprising in view of the quite different thermal histories of the specimens.

MacKenzie (1957) demonstrated that the structural state of synthetic albite, as indicated by the separation of the  $(131)$  and  $(\bar{1}\bar{3}1)$  X-ray peaks,



TABLE 5. UNIT-CELL DIMENSIONS OF AB-RICH FELDSPARS

Feldspar	composition weight per cent	$a$ (Å)	$b$ (Å)	$c$ (Å)	$\alpha$	$\beta$	$\gamma$	$V(\text{Å})_3$	$\alpha^*$	$\gamma^*$
Low Albite										
Hugo Albite										
Orville, this study	$\text{Or}_{1.7}\text{Ab}_{97.8}\text{An}_{0.2}$	8.138	12.782	7.157	94°15'	116°37'	87°42'	663.7	86°24'	90°27'
NaCl-exchanged Hugo Microcline										
Orville, this study	$\text{Or}_{1.0}\text{Ab}_{98.8}\text{An}_{0.2}$	8.142	12.781	7.155	94°05'	116°40'	87°51'	663.7	86°30'	90°22'
Ramona Albite										
Ribble, Ferguson & Taylor (1962)	$\text{Or}_{1.0}\text{Ab}_{98.8}\text{An}_{0.5}$	8.138	12.789	7.156	94°20'	116°34'	87°39'	664.2	86°20'	90°28'
Amelia Albite										
Smith (1956)	$\text{Or}_{1.8}\text{Ab}_{98.2}\text{An}_{0.0}$	8.144	12.787	7.160	94°16'	116°35'	87°40'	665.1	86°24'	90°29'
High Albite										
Synthetic Albite										
Orville, this study	$\text{Ab}_{100}$	8.151	12.862	7.115	93°39'	116°27'	89°59'	666.1	85°56'	88°12'
Donnay and Donnay (1952) <sup>1</sup>	$\text{Ab}_{100}$	8.160	12.871	7.115	93°32.5'	116°217'	90°14.1'	667.4		
Stewart, written communication 1965	$\text{Ab}_{100}$	8.160	12.870	7.106	93°33'	116°22'	90°11'	667.0	85°57'	88°02'
Heated Amelia Albite										
Ferguson, Trail and Taylor (1958)	$\text{Or}_{1.6}\text{Ab}_{97.7}\text{An}_{0.7}$	8.149	12.880	7.106	93°22'	116°18'	90°17'	666.7		
Smith (1956)	$\text{Or}_{1.8}\text{Ab}_{98.2}\text{An}_{0.0}$	8.165	12.872	7.111	93°27'	116°26'	90°19.8'	668.0	86°1'	87°58'

<sup>1</sup> 0.025° 2 $\theta$  has been added to each observation as suggested by Smith (1956, p. 537) and re-refined by computer program of Evans, Appleman and Handwerker (1963).

TABLE 6. UNIT-CELL DIMENSIONS OF OR-RICH FELDSPARS

Feldspar	Composition	<i>a</i> (Å)	<i>b</i> (Å)	<i>c</i> (Å)	$\alpha$	$\beta$	$\gamma$	<i>V</i> (Å) <sup>3</sup>	$\alpha^*$	$\gamma^*$ Triclinicity
Microcline Hugo Microcline Orville, this study Double Exchange Hugo Microcline	Or <sub>98</sub>	8.577	12.961	7.220	90°38'	115°57'	87°45'	721.2	90°23'	92°12' 0.94
Orville, this study KCl Exchange Hugo Albite	Or <sub>99.5</sub> Ab <sub>0.3</sub> An <sub>0.2</sub>	8.589	12.963	7.223	90°37'	115°57'	87°44'	722.5	90°25'	92°13' 0.96
Orville, this study Pellotsalo Microcline	Or <sub>99</sub>	8.582	12.964	7.222	90°38'	115°56'	87°41'	722.1	90°26'	92°16' 0.99
Brown and Bailey, 1964 Spencer U <sup>11</sup>	Or <sub>96</sub>	8.560	12.964	7.215	90°39'	115°50'	87°42'	720.0	90°23'	92°14' 0.96
Bailey and Taylor, 1955 Blue Mountain Microcline Stewart, written commun- 1966	Or <sub>88.9</sub> Ab <sub>12.7</sub> An <sub>1.4</sub>	8.578	12.960	7.211	90°18'	115°18'	89°08'		90°05'	90°46' 0.25
MacKenzie, 1954 Monoclinic K-feldspar Synthetic Sanidine	Or <sub>92.6</sub> Ab <sub>7.2</sub> An <sub>0.3</sub>	8.578 8.574	12.961 12.981	7.221 7.222	90°40' 90°41'	115°59' 115°59'	87°38' 87°30'	721.1	90°25' 90°18'	92°18' 0.99 92°22' 1.00
Orville, this study Donnay and Donnay, 1952 Spencer C <sup>11</sup> orthoclase	Or <sub>100</sub> Or <sub>100</sub>	8.603 8.617	13.021 13.030	7.178 7.176	90° 90°	116°01' 116°05'	90°00' 90°00'	722.6 723.7	90° 90°	0.00 0.00
Jones and Taylor, 1961 Heated Spencer C <sup>11</sup>	Or <sub>92</sub> Ab <sub>6</sub> An <sub>2</sub>	8.562	12.996	7.193	90°	116°01'	90°	719.3	90°	0.00
Cole, Sörum and Kennard, 1949	Or <sub>92</sub> Ab <sub>6</sub> An <sub>2</sub>	8.564	13.030	7.175	90°	115°59'	90°	719.6	90°	0.00

varies with the temperature and duration of hydrothermal crystallization and also depends to some degree on the grain size of the glass starting material. Albite first crystallizes with a maximum or near-maximum separation of the  $131\text{--}\bar{1}31$  peaks; the separation of these peaks decreases with time until an apparently constant value is reached which is different for each temperature in the range 700 to 1000°C. These values for the separation of  $(131)\text{--}(\bar{1}31)$  and the approximate time required to achieve them are summarized from the data of MacKenzie (1957) in Table 7. The  $(131)\text{--}(\bar{1}31)$  separation for the synthetic albite  $\text{Ab}_{100}$  crystallized in this study at 800°C for 5 days is  $1.94^\circ 2\theta$  for  $\text{CuK}\alpha$  radiation. This is very close to MacKenzie's value attained in 4 days at 800°C (Table 7) and may, as MacKenzie suggests in his study, represent the equilibrium degree of ordering at this temperature.

TABLE 7. RELATION BETWEEN  $\Delta 2\theta(131\text{--}\bar{1}31)$  AND CRYSTALLIZATION TEMPERATURE OF SYNTHETIC ALBITE ( $\text{Ab}_{100}$ ). DATA FROM MACKENZIE, (1957)

Temperature (°C)	700°	750°	800°	850°	900°	1000°
Constant $\Delta 2\theta$ (131- $\bar{1}31$ )	1.795	1.889	1.925	1.945	1.983	2.015
Time required	>50 days	10 days	4 days	2 days	1 day	<1 day

Little is known about the effect of crystallization history on the structural state of  $\text{Or}_{100}$  and intermediate members of the synthetic sanidine-high albite series. Tuttle (1952) has distinguished high and low forms of sanidine that differ in axial angle and in the orientation of the optic plane. Low sanidine has a small axial angle ( $\sim 20^\circ$ ) and its optic plane is perpendicular to (010). High sanidine has a large axial angle ( $\sim 60^\circ$  for  $\text{Or}_{100}$ ) and its optic plane is parallel to (010). Most natural sanidines belong to the low sanidine series. High sanidine has been produced from orthoclase and low sanidine by dry heating at about 1000°C and a synthetic K-feldspar crystallized hydrothermally at 800°C was found to be high sanidine (Tuttle, 1952). The  $b$  and  $c$  unit-cell dimensions of the hydrothermal sanidines produced in this study are indicative of the high sanidine series (Wright and Stewart, written communication), but the extremely fine grain size of the synthetic material make it impossible to confirm this by determining axial angle or the orientation of the optic plane.

*Microcline-low albite series.* The homogeneous K-feldspar matrix of the Hugo microcline perthite starting material was estimated above to contain about 5 percent plagioclase in solid solution. The unit cell parameters of the Hugo microcline are completely consistent with those of a

member of the prepared microcline-low albite series having 4 to 5 percent plagioclase in solution (see Figs. 3, 4, and 5). This is good evidence that the alkali exchange and homogenization treatments did not appreciably affect the structural state of the feldspar material.

It is possible that the small amount of plagioclase phase (about 7 percent) that is present as inclusions in the Hugo microcline has a somewhat different structural state from the microcline matrix phase, but the X-ray powder pattern of the exchanged and homogenized feldspars will represent that of the dominant matrix material.

In a note accompanying this paper, Rankin points out that the microcline-low albite series feldspars prepared in this study are not well-suited for optical study because of the very fine-scale grid twinning exhibited by most grains. Those few grains for which he was able to determine axial angle were coarsely twinned or untwinned. Because twin lamellae of the plagioclase inclusions are much wider than twin lamellae of the microcline matrix (0.03–0.3 mm for plagioclase versus 0.002–0.005 mm for microcline), it is likely that most, if not all, measurements of axial angle were on grains originally part of plagioclase inclusions. A typical 100–200 mesh grain would be about 0.1 mm in size and would therefore contain several thousand domains of grid twinning characteristic of the microcline matrix but only one or a few domains of lamellar twinning characteristic of the plagioclase inclusions (see Fig. 1).

The microcline-low albite series prepared in this study falls slightly toward less ordered structures from the line connecting maximum microcline and low albite on the  $\alpha$ - $\gamma$  diagram (Fig. 12). The discrepancy at the K-rich end of the series is only slightly greater than the experimental error and may not be significant, but the trend of points at the Ab-rich end of the series is definitely toward less ordered states than low albite. The difference between the structural state represented here by the prepared microcline-low albite series and that of natural low albite is further confirmed by K-exchange of the Hugo low albite. The nearly pure K-microcline produced in this way falls slightly toward more ordered structures at the Or-rich end of the prepared microcline-low albite series.

There does not seem to be any significant difference between the trend of the microcline-low albite series on the  $b$ - $c$  diagram and the generally accepted values for low albite and maximum microcline. It is clear, however, that the  $\alpha$ - $\gamma$  plot is much more sensitive to variations in structural state of the triclinic Or-rich feldspars than the  $b$ - $c$  plot. Note the large difference between "Spencer U" and maximum microcline on the  $\alpha$ - $\gamma$  diagram (Fig. 12) versus the relatively small difference on the  $b$ - $c$  diagram (Figure 11).

*Effect of composition and structural state on "triclinicity."* Composition (in the range Or<sub>100</sub> to Or<sub>70</sub>Ab<sub>30</sub>) has only a small effect on  $\gamma$  and  $\gamma^*$  for microcline of high obliquity. It is useful, therefore, to use  $\gamma$ ,  $\gamma^*$  or some property directly related to  $\gamma^*$ , as a measure of structural state.

MacKenzie (1954) proposed that separation of the peaks (130) and ( $\bar{1}30$ ) be used as a measure of structural state since it is almost entirely a function of  $\gamma^*$  (as are all pairs of peaks of the type  $(h\bar{k}0) - (\bar{h}k0)$ ). Unfortunately, (130) is very near (200) which in at least some microcline specimens has nearly equal intensity. In many natural microcline powder patterns (200) and (130) combine to make a single unresolved peak. There does not seem to be any other suitable pair of strong peaks of this type.

Goldsmith and Laves (1954) relate the degree of order in microcline

TABLE 8.  $\Delta$ -VALUES FOR OR-RICH MEMBERS OF MICROCLINE-LOW ALBITE SERIES  
 $\Delta = 12.5 [d(131) - d(\bar{1}31)]$

Composition Mol %	Or <sub>99.5</sub>	Or <sub>89.6</sub>	Or <sub>79.8</sub>	Or <sub>70.0</sub>
Predicted $\Delta$ -values <sup>1</sup>	0.956	0.917	0.871	0.791
Observed $\Delta$ -values <sup>2</sup>	0.940	0.906	0.876	0.782

<sup>1</sup> Calculated from unit cell dimensions given in Table 3.

<sup>2</sup> Calculated from observed positions of 131 and  $\bar{1}31$  peaks.

feldspars to the deviation of both  $\alpha$  and  $\gamma$  (or  $\alpha^*$  and  $\gamma^*$ ) from 90°. The amount of this deviation they call "triclinicity" and suggest that the difference in spacing of the peaks (131) and ( $\bar{1}31$ ) be taken as a measure of triclinicity and of the degree of order. They define a measure of triclinicity,  $\Delta$ , as follows:

$$\Delta = 12.5[d(131) - d(\bar{1}31)]$$

so that a microcline with the maximum observed difference  $d(131) - d(\bar{1}31)$  has a  $\Delta$ -value of approximately unity. The  $\Delta$ -value, however, varies with both Al:Si order and composition. The effect of composition on  $\Delta$ -values at constant Al:Si order is shown in Table 8. Close agreement is shown in Table 8 between  $\Delta$ -values predicted from unit-cell dimensions and those based upon observed positions of the (131) and ( $\bar{1}31$ ) peaks. This suggests that  $\Delta$ -values determined for natural microclines are a valid measure of Al:Si order providing that the effect of composition is taken into account.

The combined effects of composition and structural state on the  $\Delta$ -value have been plotted in the microcline region of an  $\alpha$ - $\gamma$  diagram (Fig. 13). The series of microcline-low albite compositions produced in this study have been shown to constitute a line of constant (although prob-

ably not the lowest) structural state. This line correlates varying  $\Delta$ -values and Or-contents. It is drawn as a dashed line in Figure 13. The large circles in Figure 13 represent members of the prepared microcline-low albite series and the inserted figures correspond to Or-contents given in Table 8. Analogous lines of constant structural state have been found to be approximately parallel to this series (Wright, 1964; Stewart, written communication). Intermediate microclines of Or<sub>100</sub> composition should

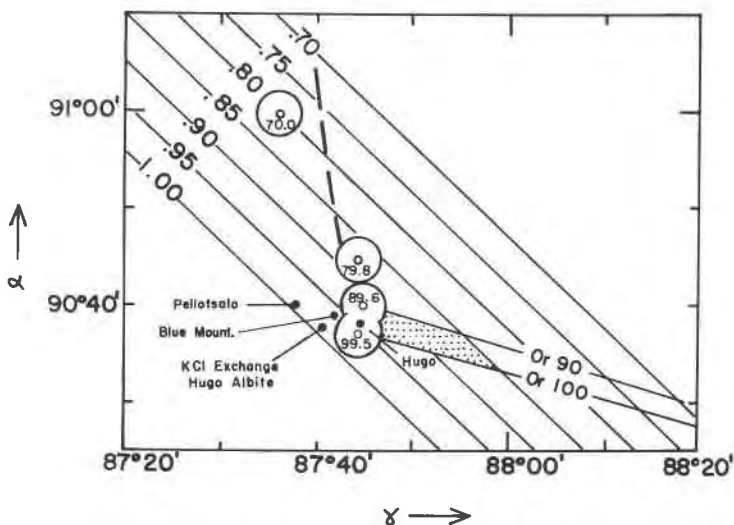


FIG. 13. Maximum microcline region of  $\alpha$ - $\gamma$  plot. Lines of constant "triclinicity" ( $\Delta$ -values) shown. Stipled area includes most microclines for which  $\Delta$ -values were determined by Dietrich (1962). Small closed circles represent microcline specimens from Table 6. Large open circles represent members of prepared microcline-low albite series and the inserted figures correspond to Or-contents given in Table 8.

fall along the line between Or<sub>100</sub> sanidine and Or<sub>100</sub> microcline. Other lines of variable structural state but constant composition will probably be nearly parallel to this line.

Dietrich (1962) has determined the  $\Delta$ -value of 500 alkali feldspars from a wide variety of geologic environments. This data gives some indication of the structural state of the geologically abundant microcline when it is interpreted with the aid of Figure 12. Somewhat over a half of the 500 samples have  $\Delta$ -values greater than 0.80 and two thirds of these fall in the range of 0.85 to 0.95. If we assume that Or<sub>100</sub> to Or<sub>90</sub>Ab<sub>10</sub> represents the composition range of natural microcline, "common" microcline is concentrated in the area of Figure 13 bounded by these composition lines and by  $\Delta$ -value lines 0.85 and 0.95. It would seem to follow from this that

most natural microclines are in a somewhat less ordered structural state than the microcline-low albite series prepared in this study.

*Acknowledgements.* This work was supported by NSF grants GP398 and GP4484. I am grateful to the U. S. Geological Survey for unit-cell and curve-fitting calculations run on their computer, and particularly grateful to D. B. Stewart, of the U. S. Geological Survey, who has aided this work in many ways.

## REFERENCES

- BAILEY, S. W. AND W. H. TAYLOR (1955) The structure of a triclinic potassium feldspar. *Acta Crystallogr.* **8**, 621-632.
- BOWEN, N. L. AND O. F. TUTTLE (1950) The system  $\text{NaAlSi}_3\text{O}_8$ - $\text{KAlSi}_3\text{O}_8$ - $\text{H}_2\text{O}$ . *J. Geol.* **58**, 489-511.
- BROWN, B. E. AND S. W. BAILEY (1964) The structure of maximum microcline. *Acta Crystallogr.* **17**, 1391-1400.
- COLE, W. F., SØRUM AND O. KENNARD (1949) The crystal structures of orthoclase and sanidinized orthoclase. *Acta Crystallogr.* **2**, 280-287.
- DIETRICH, R. V. (1962) K-feldspar structural states as petrogenetic indicators. *Norsk Geol. Tidsskr.* **42**, pt. 2, 394-414.
- DONNAY, G. AND J. D. H. DONNAY (1952) The symmetry change in the high-temperature alkali-feldspar series. *Amer. J. Sci.*, Bowen Volume, p. 115-132.
- EVANS, H. T., JR., D. E. APPLEMAN AND D. S. HANDWERKER (1963) The least squares refinement of crystal unit cells with powder diffraction data by an automatic computer indexing method (abs.). *Amer. Crystallogr. Ass. Meeting* Cambridge, Mass., March 28, 1963, p. 42-43.
- FERGUSON, R. B., R. J. TRAILL AND W. H. TAYLOR (1958) The crystal structure of low-temperature and high-temperature albites. *Acta Crystallogr.* **11**, 331-348.
- FYFE, W. S., TURNER, F. J. AND J., VERHOOGEN, (1958), Metamorphic reactions and metamorphic facies. *Geol. Soc. Amer. Mem.* **73**, 259 p.
- GOLDSMITH, J. R. AND F. LAVES (1954) The microcline-sanidine stability relations. *Geochim. et Cosmochim. Acta* **5**, 1-19.
- (1961) The sodium content of microclines and the microcline-albite series. *Cursillos Conf. Inst. Lucas Mallada* **8**, 81-96.
- GOLDSTEIN, D. (1959) A new indicator for the complexometric determination of calcium. *Anal. Chim. Acta* **21**, 339-340.
- JONES, J. B. AND W. H. TAYLOR (1961) The structure of orthoclase. *Acta Crystallogr.* **14**, 443-456.
- LAVES, F. (1951) Artificial preparation of microcline. *J. Geol.* **59**, 511-512.
- (1952a) Phase relations of the alkali feldspars—I. *J. Geol.* **60**, 436-449.
- (1952b) Phase relations of the alkali feldspars—II. *J. Geol.* **60**, 549-574.
- MACKENZIE, W. S. (1954) The orthoclase-microcline inversion. *Mineralog. Mag.* **30**, 543-366.
- (1957) The crystalline modifications of  $\text{NaAlSi}_3\text{O}_8$ . *Amer. J. Sci.* **255**, 481-516.
- NORTON, J. J., L. R. PAGE AND D. A. BROBST (1962) Geology of the Hugo pegmatite, Keystone, South Dakota. *U.S. Geol. Surv. Prof. Pap.* **297-B**, 49-127.
- ORVILLE, P. M. (1960) Powder X-ray method for determination of (Ab+An) content of microcline. *Geol. Soc. Amer. Bull.* **71**, 1939-1940.

- (1963) Alkali ion exchange between vapor and feldspar phases. *Amer. J. Sci.* **261**, 201–237.
- RIBBE, P. H., R. B. FERGUSON AND W. H. TAYLOR (1962) A three-dimensional refinement of the structure of low albite. *Norsk Geol. Tidsskr.* **42**, 152–157.
- SMITH, J. V. (1956) The powder patterns and lattice parameters of plagioclase feldspars. I. The soda-rich plagioclases. *Mineral. Mag.* **31**, 47–68.
- (1961) Explanation of strain and orientation effect sin perthites. *Amer. Mineral.* **46**, 1489–1493.
- AND S. W. BAILEY (1963) Second review of Al-O and Si-O tetrahedral distances. *Acta Crystallogr.* **16**, 801–811.
- AND W. S. MACKENZIE (1955) The alkali feldspars: II. A simple x-ray technique for the study of alkali feldspars. *Amer. Mineral.* **40**, 733–747.
- STEWART, D. B. AND DORA VON LIMBACK (1967) Thermal expansion of low and high albite. *Amer. Mineral.* **52** (in press).
- TUTTLE, O. F. (1952) Optical studies on alkali feldspars. *Amer. J. Sci.*, Bowen Volume, 553–567.
- WRIGHT, T. L. (1964) X-ray determination of composition and structural state of alkali feldspars (abs.). *Trans. Am. Geophy. Union* **45**, 127.
- WYART, JEAN AND G. SABATIER (1956) Transformations mutuelles des feldspars alcalins; reproduction du microcline et de l'albite. *Bull. Soc. Franc. Mineral.* **79**, 444–448.

*Manuscript received, March 28, 1966; accepted for publication, November 5, 1966.*